Dalton Transactions

COMMUNICATION

U– to Z–shape isomerization in Pt_2Ag_2 framework containing pyridyl-NHC ligands

Received 00th January 20xx,
Accepted 00th January 20xx

DOI: 10.1039/x0xx00000x

rsc.li/dalton

Shinnosuke Horiuchi,[a] Sangjoon Moon,[a] Eri Sakuda,[a] Akitaka Ito,[b] Yasuhiro Arikawa,[a] Keisuke Umakoshi*[a]

Synthesis and isomerization of heteropolynuclear Pt_2Ag_2 complex containing pyridyl N-heterocyclic carbene (NHC) ligands are reported. The Pt_2Ag_2 complex could take two geometrical isomers possessing twisted U-shaped structure and Z-shaped structure. The rate of isomerization reaction depended on the concentration of the solution, implying that the reaction took place through an intermolecular process.

Metal–metal interactions have been increasingly recognized as a powerful tool to construct supramolecular and crystal engineering systems.[1] In particular, metal-metal interactions among different metal atoms are expected to show characteristic features owing to their cooperative effects, giving unique structures, reactivities, and properties. For example, bimetallic interactions in cooperative catalysis offers the unique advantage of metal centers accompanying different nature in close proximity, leading to a significant molecular activation that individual mononuclear complexes can not achieve.[2] Furthermore, structures and photophysical properties of heteropolynuclear complexes involving metal–metal interactions, such as Pt complexes containing group 11 metal ions, have also been widely investigated.[3] Some of heteropolynuclear complexes having metal–metal interactions also show unique molecular rearrangements in solution, owing to their weak bonding nature.[4]

We have revealed the structures and luminescent properties of heteropolynuclear complexes having various extent of multiple metal–metal interactions.[5] For example, $[(ppy)Pt_2Ag_2(\mu\text{-}Me_2pz)_4]$ (ppy = 2-phenylpyridinate and Me_2pz = 3,5-dimethylpyrazolate) and $[(bpy)Pt_2M_2(\mu\text{-}Me_2pz)_4](PF_6)_2$ (M = Au, Ag and bpy = 2,2'-bipyridine) exist as a mixture of U- and Z-shaped isomers in solution, respectively, whose luminescent properties are almost independent on the incorporated group 11 metal ions. Furthermore, U-shaped isomer showed reversible trapping of Ag ion within a U-shaped cavity via multiple metal–metal interactions.[5e] Although various properties of heteropolynuclear complexes have been investigated by using a variety of C^N chelate ligands represented by ppy and its derivatives, those of heteropolynuclear complexes involving N-heterocyclic carbene (NHC) ligands have not been fully explored.[6] Furthermore, structural isomerization involving rearrangement of complex framework such as that between U- and Z-shaped structures is still unclear. Herein we report the synthesis, structure, isomerization and emission properties of pyrazolato-bridged Pt_2Ag_2 complexes having pyridyl-NHC chelate ligand. The pyridyl-NHC ligand works as a neutral C^N chelate ligands similarly to N^N chelate ligands (e.g. bipyridines) and has unique electron donating character on the carbene moiety. The strong s-donor property of the NHC ligands was expected to raise the d-d transition energy effectively, resulting in a higher energy emission from the complexes.[7] In this paper, we also elucidated the nature of pyridyl-NHC ligand as a neutral C^N chelate ligand in the Pt_2Ag_2 system.

The pyrazolato-bridged Pt_2Ag_2 complex **3** was synthesized from the mononuclear Pt(II) complex **1** in a similar manner to our previous methods (Scheme 1).[5d] The dimethylpyrazolato complex $[(Py\text{-}NHC)Pt(Me_2pzH)_2](PF_6)_2$ (**2**) was obtained by the reaction of $[(Py\text{-}NHC)PtCl_2]$ (**1**) with Me_2pzH in the presence of $AgPF_6$ in CH_3CN in 75% yield. The formation of $[\mathbf{2}](PF_6)_2$ was confirmed by

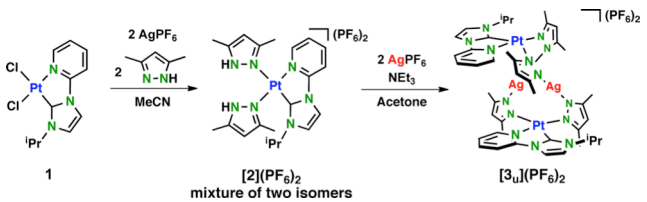

Scheme 1 Synthesis of Heteropolynuclear Pt_2Ag_2 Complex $[\mathbf{3}](PF_6)_2$

[a] *Division of Chemistry and Materials Science, Graduate School of Engineering, Nagasaki University, 1-14, Bunkyo-machi, Nagasaki 852-8521, Japan. E-mail: kumks@nagasaki-u.ac.jp*
[b] *Graduate School of Engineering/School of Environmental Science and Engineering, Kochi University of Technology, 185 Miyanokuchi, Tosayamada, Kami, Kochi 782-8502, Japan.*

†Electronic supplementary information (ESI) available: Details of experimental procedures, spectroscopic data, X-ray data and DFT calculations (PDF). For ESI and crystallographic data in CIF or other electronic format see DOI: 10.1039/x0xx00000x

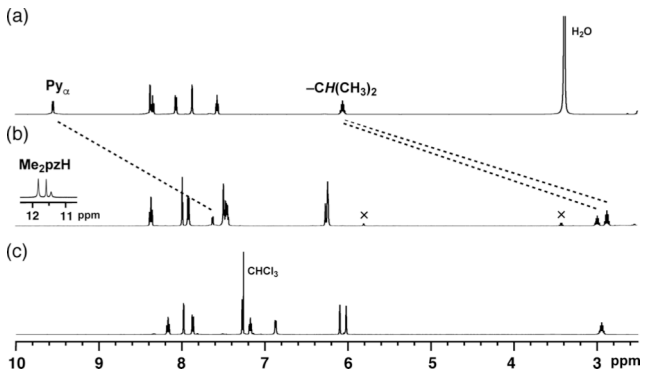

Fig. 1 ^{1}H NMR spectra (500 MHz, r.t.) of (a) **1** in DMSO-d_6, (b) [**2**]$(PF_6)_2$ consisting of two geometrical isomers in CD_3CN and (c) U-shaped Pt_2Ag_2 complex [$\mathbf{3_U}$]$(PF_6)_2$ in $CDCl_3$.

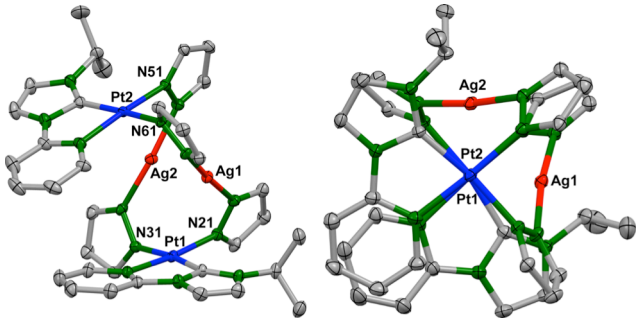

Fig. 2 ORTEP representation (50% probability ellipsoids) of U-shaped Pt_2Ag_2 complex cation [$\mathbf{3_U}$]$^{2+}$: (left) side view, (right) viewed along the Pt···Pt axis. Hydrogen atoms and methyl groups are omitted for clarity. Selected bond lengths (Å): Pt1···Pt2 5.3613(5), Pt1···Ag1 3.1537(5), Pt1···Ag2 3.5849(6), Pt1–N21 1.998(3), Pt1–N31 2.053(3), Pt2···Ag1 3.6208(5), Pt2···Ag2 3.1885(5), Pt2–N51 2.001(3), Pt2–N61 2.050(3), Ag1···Ag2 3.0745(5).

the elemental analysis and FAB mass spectrometry. The ^{1}H NMR spectrum of [**2**]$(PF_6)_2$ showed upfield shifts ($\Delta\delta$ = –2 ~ –3 ppm) of the tertiary proton at the ^{i}Pr group and the Pyα proton owing to the shielding effect from Me_2pzH moieties, indicating that the ^{i}Pr proton and the Pyα proton were perpendicularly oriented to the center of each different pyrazole rings, respectively, in solution (Fig. 1). These signals were derived from two stereoisomers having syn- and anti-conformations at pyrazole moieties (Scheme S1†). The structure of the anti-isomer of [**2**]$(PF_6)_2$ was undoubtedly confirmed by single crystal X-ray structure analysis (Fig. S10†), though the dissolution of single crystal of [**2**]$(PF_6)_2$ into CH_3CN gave a thermodynamic equilibrium state within 5 min.

The reaction of the isomer mixture of [**2**]$(PF_6)_2$ with $AgPF_6$ in a 1:1 ratio in the presence of Et_3N afforded dicationic Pt_2Ag_2 complex having Py-NHC chelate ligands and pyrazolate bridges in 64% yield. Electrospray Ionization (ESI) mass analysis clearly revealed the formation of [**3**]$(PF_6)_2$ at m/z 1504.7 which was assigned to $[M–(PF_6)]^+$ fragments. The molecular structure of [**3**]$(PF_6)_2$ was determined by single crystal X-ray structure analysis.

A colorless single crystal of [**3**]$(PF_6)_2$ suitable for X-ray structure analysis was obtained from acetone-hexane solution of [**3**]$(PF_6)_2$. The X-ray structure analysis revealed that complex cation in the crystal has twisted U-shaped structure (Fig. 2); hereafter [$\mathbf{3_U}$]$^{2+}$ and [$\mathbf{3_Z}$]$^{2+}$ denote the complex cation having U-shaped structure and Z-shaped structure, respectively. The view along Pt•••Pt axis of [$\mathbf{3_U}$]$^{2+}$ shows that the pyridine rings in each Py-NHC ligand take eclipsed configuration probably due to the steric hindrance of isopropyl substituents on each NHC ligand. The tertiary protons of isopropyl groups at NHC ligands located above the bridging pyrazolato ligands, suggesting that CH–π interactions may contribute to the formation of the Pt_2Ag_2 structure.[8] The larger deviation in Pt•••Ag distances (3.1537(5), 3.1885(5), 3.5849(6), 3.6208(5) Å) in [$\mathbf{3_U}$]$^{2+}$ implies more distorted structure of [$\mathbf{3_U}$]$^{2+}$ compared with Pt_2Ag_2 analogue having ppy chelate ligands, $[Pt_2Ag_2(ppy)_2(Ph_2pz)_4]$ (Pt•••Ag, 3.2028(5), 3.4249(3) Å).[5d,e] These metal–metal distances are shorter than the sum of the van der Waals radius of the metal atoms (Pt: 1.77 Å, Ag: 1.65 Å), suggesting the existence of cooperative metal–metal interactions in [$\mathbf{3_U}$]$^{2+}$. In contrast, the complex cations and the counter anions were alternately oriented in the crystal, indicating no intermolecular metal–metal interaction in the solid state (Fig. S11†). The Pt–$N_{pyrazolato}$ bond distances at trans position of NHC moieties are approximately 0.05 Å longer than those at trans position of pyridine rings. The difference is attributed to the stronger trans influence of NHC moiety than that of pyridine moiety.

The NMR studies revealed that the U-shaped Pt_2Ag_2 complex [$\mathbf{3_U}$]$^{2+}$ showed isomerization in the solution, although multiple metal–metal interactions were observed in the crystal structure (Fig. 3a). When the single crystal of the U-shaped isomer [$\mathbf{3_U}$]$(PF_6)_2$ was dissolved in $CDCl_3$, new sets of the signals appeared within 5 min and their intensities gradually increased (Fig. S6†). The signals assigned to pyridine protons were observed around a downfield region compared with those of [$\mathbf{3_U}$]$^{2+}$, suggesting that Py-NHC ligands of the new species were not stacked each other. This behavior is very similar to those of Pt_2Ag_2 analogues, which exist as a mixture of U- and Z-shaped complex in the solution.[5d] Thus the new sets of signals in the ^{1}H NMR spectrum were assigned to the Z-shaped isomer [$\mathbf{3_Z}$]$^{2+}$. In addition, the integral ratios of the signals reached U:Z = 2:1 in a thermodynamic equilibrium state (Fig. 3b). These results suggest that the metal–metal interactions and Ag–$N_{pyrazolato}$ bonds in [**3**]$^{2+}$ are actually labile in solution. The U-shaped isomer is thermodynamically favored one as evidenced by the integral ratio of U:Z in ^{1}H NMR spectra, probably because the highly twisted U-shaped structure can induce the short contacts among the Pt and Ag ions to endow effective thermodynamic stability by metal–metal interaction. These two sets of signals for [$\mathbf{3_U}$]$^{2+}$ and [$\mathbf{3_Z}$]$^{2+}$ were also observed in the crude reaction product (Fig. S8†). Thus, the U-shaped isomer [$\mathbf{3_U}$]$(PF_6)_2$ was selectively crystallized via isomerization in the crystallization process. It is noteworthy here that the isomerization rate became slow in a diluted condition, indicating that the reaction took place through an intermolecular process (Fig. 3b). Additionally, the isomerization reaction immediately reached a state of thermodynamic equilibrium when single crystals of the U-shaped isomer [$\mathbf{3_U}$]$(PF_6)_2$ was dissolved in coordinating solvent, such as CD_3CN. It implies that isomerization was accelerated by the coordination of solvent molecules to the Ag ions, which was competed with that of Me_2pz ligands. The VT-NMR spectra of [**3**]$^{2+}$ (*i.e.* the mixture of [$\mathbf{3_U}$]$^{2+}$ and [$\mathbf{3_Z}$]$^{2+}$ in the state of thermodynamic equilibrium) recorded even at

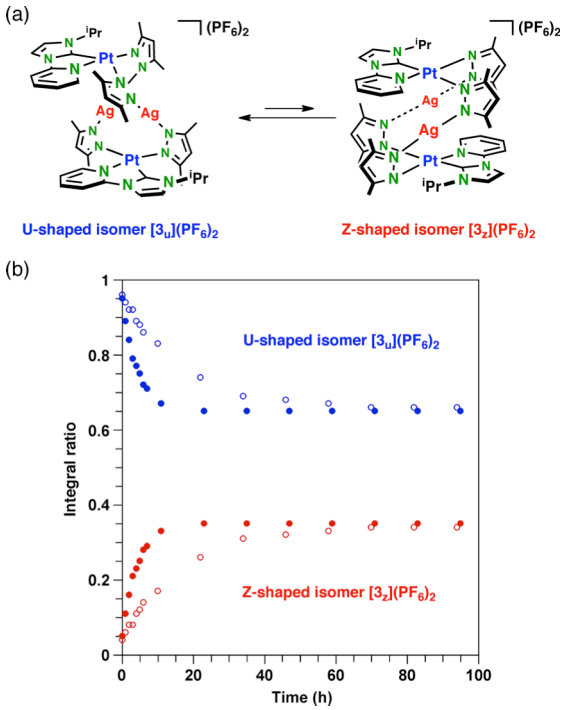

Fig. 3 a) Schematic representation of the isomerization from U-shaped isomer $[\mathbf{3_U}](PF_6)_2$ to Z-shaped isomer $[\mathbf{3_Z}](PF_6)_2$. b) The variation with time of the relative value of the integrated intensities H_4 in $[\mathbf{3_U}]^{2+}$ (δ = 8.17 ppm) and $[\mathbf{3_Z}]^{2+}$ (δ = 8.34 ppm), which are proportional to the concentration of $[\mathbf{3_U}]^{2+}$ and $[\mathbf{3_Z}]^{2+}$, respectively, after single crystals of $[\mathbf{3_U}](PF_6)_2$ were dissolved in $CDCl_3$ in dark at 25°C (circles, 15 mM; hollow circles, 6 mM).

313 K in $CDCl_3$ and CD_3CN showed no coalescence of signals, indicating that isomerization between U- and Z-shaped structure is slow process and does not proceed in the NMR time scale (Fig. S7†).

We recently reported that U-shaped Pt_2Ag_2 complexes having C^N chelate ligands can show reversible entrapment of Ag(I) ion in the Pt_2Ag_2 framework through Ag•••Ag interaction and the formation of Pt→Ag dative bonds.[5e] Therefore, the U-shaped Pt_2Ag_2 structure of $[\mathbf{3_U}](PF_6)_2$ encouraged us to elucidate a binding ability for Ag(I) ion in solution. However, the ^{1}H NMR spectrum of $[\mathbf{3}]^{2+}$ did not change even by the addition of the excess amount of Ag(I) ion into the solution, indicating that the U-shaped Pt_2Ag_2 complex $[\mathbf{3_U}]^{2+}$ can not stabilize additional Ag(I) ion in the Pt_2Ag_2 framework via multiple metal–metal interactions (Fig. S9†). On the other hand, Miguel recently reported that a dicationic $[Ag_2(bisNHC)_2]^{2+}$ complex captures even cationic $[Ag(NCCH_3)_2]^+$ guest in the molecular cavity of Ag_2 framework via strong argentophilic interactions, which overcomes the electrostatic repulsion between the complex cation and Ag ion.[9] These results strongly suggest that a π–coordination ability of C(ipso) atom in the C^N chelate ligand plays an important role for the capturing of Ag(I) ion into the Pt_2Ag_2 systems through Ag-C(ipso) bonding interaction. The lack of π-coordination ability of the carbene carbon atom in Py-NHC ligand is attributed to the insensitive behavior of $[\mathbf{3_U}]^{2+}$ toward Ag(I) ion.

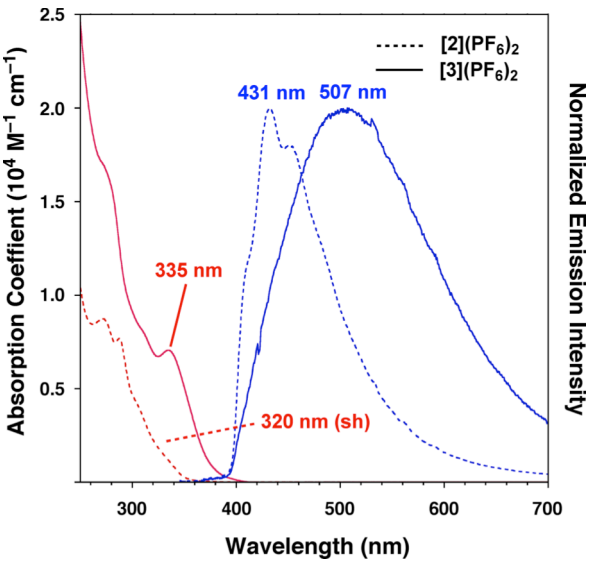

Fig. 4 UV-Vis absorption spectra (red) of $[\mathbf{2}](PF_6)$ (dash line) and $[\mathbf{3}](PF_6)_2$ (solid line) in CH_3CN and their normalized emission spectra (blue) in the solid state at room temperature (λ_{ex} = 355 nm).

The mononuclear Pt(II) complex $[\mathbf{2}](PF_6)_2$ and Pt_2Ag_2 complex $[\mathbf{3}](PF_6)_2$ showed the lowest energy absorption bands at 320 nm (sh) and 335 nm, respectively, in CH_3CN at room temperature, whose energies are higher than those of Pt_2Ag_2 analogue having ppy chelate ligands (Fig. 4).[5d] Since the corresponding absorption band is absent in $[\mathbf{2}](PF_6)_2$, the band at 335 nm in $[\mathbf{3}](PF_6)_2$ is originated from the formation of Pt_2Ag_2 structure.

Although the complexes $[\mathbf{2}](PF_6)_2$ and $[\mathbf{3}](PF_6)_2$ did not display photoluminescence in solution at room temperature, they showed structured emission spectrum (λ_{max} = 431 nm) and broad one (λ_{max} = 507 nm), respectively, in the solid state (Fig. 4). The observed lifetimes of the emission in few hundreds of nanoseconds indicate that the emissions are phosphorescence (Table S1†). Corresponding to the appearance of lower energy absorption bands in $[\mathbf{3}](PF_6)_2$, the emission bands of $[\mathbf{3}](PF_6)_2$ significantly red-shifted ($\Delta\lambda_{max}$ = +76 nm) compared with those of $[\mathbf{2}](PF_6)_2$, indicating that the incorporation of Ag(I) ions drastically affects the emission energy. To our surprise, the emission quantum yield (Φ) of $[\mathbf{3}](PF_6)_2$ (1%) was smaller than that of $[\mathbf{2}](PF_6)_2$ at room temperature. This is in contrast to our previous results that the formation of mixed-metal complexes having multiple metal–metal interactions affords brighter luminescence than the precursor Pt(II) complex in the solid states.[5]

To unveil the origin of the differences in photophysical properties between $[\mathbf{2}](PF_6)_2$ and $[\mathbf{3}](PF_6)_2$, the time dependent density functional theory (TD-DFT) method were investigated. The DFT calculation clearly visualized the highest-occupied molecular orbitals (HOMOs) and lowest-unoccupied molecular orbitals (LUMOs) in the complexes (Tables S3–S6, Fig. S13 and S14†). LUMOs of the both complexes are similar to each other and consisting of the π* orbital of pyridyl moiety, while HOMOs are consisting of π orbital of Me_2pz moieties and 5d orbital of Pt atom. Moreover, large contribution of 4d orbital of Ag atoms is found in HOMO-2 of $[\mathbf{3}](PF_6)_2$. These calculations suggest that the lowest energy

absorption bands of [**2**](PF$_6$)$_2$ can be assigned mainly to the combination of ligand-to-ligand charge transfer (LLCT) [Me$_2$pz → π*(Py-NHC)] and metal-to-ligand charge transfer (MLCT) [Pt → π*(Py-NHC)] transitions. The assignment for [**3**](PF$_6$)$_2$ is essentially very similar to that of [**2**](PF$_6$)$_2$. However, in addition to the combination of LLCT and MLCT transitions, the metal-to-ligand charge transfer (M'LCT) [Ag → π*(Py-NHC)] transitions further contribute to the lowest energy absorption band in [**3**](PF$_6$)$_2$ due to the formation of Pt$_2$Ag$_2$ complex. The features of emission spectra of [**2**](PF$_6$)$_2$ and [**3**](PF$_6$)$_2$ may be attributed to the different nature of their excited states (Tables S5 and S6†).

Conclusions

In summary, we synthesized the heteropolynuclear Pt$_2$Ag$_2$ complex having pyridyl-NHC chelating ligands with multiple Pt–Ag and Ag–Ag interactions. Although the as-prepared Pt$_2$Ag$_2$ complex exists as a mixture of two isomers, it selectively crystalized to afford only U-shaped isomer in the solid state, allowing us to elucidate the thermodynamically favored isomer as well as the U to Z structural isomerization in solution. The Pt$_2$Ag$_2$ complex having pyridyl-NHC chelating ligands showed higher emission energy than the Pt$_2$Ag$_2$ analogues having other aromatic C^N chelate ligands like 2-phenylpyridine derivatives. This is probably due to the strong σ-donating ability of carbene carbon atom on the Py-NHC ligand. These results give us new insights into the relationship between structural transformations and photophysical properties involving weak intramolecular metal–metal interactions, leading to a construction of new types of functional molecules incorporating both dynamic molecular systems and light-emitting properties.

Conflicts of interest

There are no conflicts to declare.

Acknowledgements

This work was partially supported by JSPS KAKENHI grant numbers 15K05456 and 17K14463 and Nippon Sheet Glass Foundation for Materials Science and Engineering.

Notes and references

1 (a) C.-M. Che, S.-W. Lai, *Coord. Chem. Rev*., 2005, **249**, 1296; (b) H. Schmidbaur, A. Schier, *Chem. Soc. Rev*., 2012, **41**, 370; (c) H. Schmidbaur, A. Schier, *Angew. Chem. Int. Ed*., 2015, **54**, 746; (d) H. Schmidbaur, A. Schier, *Organometallics*, 2015, **34**, 2048; (e) V. W.-W. Yam, V. K.-M. Au, S. Y.-L. Leung, *Chem. Rev*., 2015, **115**, 7589; (f) M. Yoshida, M. Kato, *Coord. Chem. Rev*., 2018, **355**, 101.

2 (a) M. H. Pérez-Temprano, J. A. Casares, P. Espinet, *Chem Eur. J*., 2012, **18**, 1864; (b) P. Buchwalter, J. Rosé, P. Braunstein, *Chem. Rev*., 2015, **115**, 28; (c) N. P. Mankad, *Chem. Eur. J.,* 2016, **22**, 5822; (d) I. G. Powers, C. Uyeda, *ACS Catal*., 2017, **7**, 936.

3 (a) R. Buschbeck, P. J. Low, H. Lang, *Coord. Chem. Rev.,* 2011, **255**, 241; (b) Á. Díez, E. Lalinde, M. T. Moreno, *Coord. Chem. Rev*., 2011, **255**, 2426; (c) T. Yamaguchi, F. Yamazaki, T. Ito, *J. Am. Chem. Soc.,* 2001, **123**, 743; (d) D. E. Janzen, L. F. Mehne, D. G. VanDerveer, G. J. Grant, *Inorg. Chem*., 2005, **44**, 8182; (e) M.-E. Moret, P. Chen, *J. Am. Chem. Soc*., 2009, **131**, 5675; (f) S. Jamali, Z. Mazloomi, S. M. Nabavizadeh, D. Milić, R. Kia, M. Rashidi, *Inorg. Chem*., 2010, **49**, 2721; (g) S. Fuertes, C. H. Woodall, P. R. Raithby, V. Sicilia, *Organometallics*, 2012, **31**, 4228; (h) X. Zhang, B. Cao, E. J. Valente, T. K. Hollis, *Organometallics*, 2013, **32**, 752; (i) K. Kubo, H. Okitsu, H. Miwa, S. Jume, R. G. Cavell, T. Mizuta, *Organometallics*, 2017, **36**, 266.

4 (a) N. Oberbeckmann-Winter, X. Morise, P. Braunstein, R. Welter, *Inorg. Chem.,* 2005, **44**, 1391; (b) J. Forniés, C. Fortuño, S. Ibáñez, A. Martín, P. Mastrorilli, V. Gallo, *Inorg. Chem*., 2011, **50**, 10798; (c) N. Bebra, S. Ladeira, L. Maron, B. Bartin-Vaca, D. Bourissou, *Chem. Eur. J*., 2012, **18**, 8474; (d) M. Baya, Ú. Belío, I. Fernández, S. Fuertes, A. Martín, *Angew. Chem. Int. Ed*., 2016, **55**, 6978.

5 (a) K. Umakoshi, T. Kojima, K. Saito, S. Akatsu, M. Onishi, S. Ishizaka, N. Kitamura, Y. Nakao, S. Sakaki, Y. Ozawa, *Inorg. Chem*., 2008, **47**, 5033; (b) K. Umakoshi, K. Saito, Y. Arikawa, M. Onishi, S. Ishizaka, N. Kitamura, Y. Nakao, S. Sakaki, *Chem. Eur. J*., 2009, **15**, 4238; (c) S. Akatsu, Y. Kanematsu, T. Kurihara, S. Sueyoshi, Y. Arikawa, M. Onishi, S. Ishizaka, N. Kitamura, Y. Nakao, S. Sakaki, K. Umakoshi, *Inorg. Chem*., 2012, **51**, 7977; (d) K. Nishihara, M. Ueda, A. Higashitani, Y. Nakao, Y. Arikawa, S. Horiuchi, E. Sakuda, K. Umakoshi, *Dalton Trans.,* 2016, **45**, 4978; (e) M. Ueda, S. Horiuchi, E. Sakuda, Y. Nakao, Y. Arikawa, K. Umakoshi, *Chem. Commun*., 2017, **53**, 6405.

6 Z. Han, J. I. Bates, D. Strehl, B. O. Patrick, D. P. Gates, *Inorg. Chem.,* 2016, **55**, 5071.

7 (a) C.-S. Lee, S. Sabiah, J.-C. Wang, W.-S. Hwang, I. J. B. Lin, *Organometallics*, 2010, **29**, 286; (b) C.-S. Lee, R. R. Zhuang, S. Sabiah, J.-C. Wang, W.-S. Hwang, I. J. B. Lin, *Organometallics*, 2011, **30**, 3897; (c) Y. Zhang, J. A. Garg, C. Michelin, T. Fox, O. Blacque, K. Venkatesan, *Inorg. Chem*., 2011, **50**, 1220; (d) S. Y.-L. Leung, E. S.-H. Lam, W. H. Lam, K. M.-C. Wong, W.-T. Wong, V. W.-W. Yam, *Chem. Eur. J*., 2013, **19**, 10360; (e) Y. Zhang, C. Clavadetscher, M. Bachmann, O. Blacque, K. Venkatesan, *Inorg. Chem*., 2014, **53**, 756; (f) P. Pinter, H. Mangold, O. Stengel, I. Münster, T. Strassner, *Organometallics*, 2016, **35**, 673; (g) M. Bachmann, D. Suter, O. Blacque, K. Venkatesan, *Inorg. Chem*., 2016, **55**, 4733; (g) H. Leopold, M. Tenne, A. Tronnier, S. Metz, I. Münster, G. Wagenblast, T. Strassner, *Angew. Chem. Int. Ed*., 2016, **55**, 15779.

8 (a) M. Nishio, Y. Umezawa, M. Hirota, Y. Takeuchi, *Tetrahedron*, 1995, **32**, 8665; (b) O. Takahashi, Y. Konno, M. Nishio, *Chem. Rev*., 2010, **110**, 6049.

9 (a) A. Vellé, A. Cebollada, M. Iglesias, P. J. S. Miguel, *Inorg. Chem*., 2014, **53**, 10654; (b) A. Cebollada, A. Vellé, M. Iglesias, L. B. Fullmer, S. Goberna-Ferrón, M. Nyman, P. J. S. Miguel, *Angew. Chem. Int. Ed*., 2015, **54**, 12762.

